Electronic Supplementary Information for

Bimetallic Ag_3Cu porous networks for ambient electrolysis of nitrogen to ammonia

Hongjie Yu, Ziqiang Wang,* Dandan Yang, Xiaoqian Qian, You Xu, Xiaonian Li,

Hongjing Wang* and Liang Wang*

State Key Laboratory Breeding Base of Green-Chemical Synthesis Technology, College of Chemical Engineering, Zhejiang University of Technology, Hangzhou 310014, P. R. China

*Corresponding authors' E-mails: zqwang@zjut.edu.cn; hjw@zjut.edu.cn; wangliang@zjut.edu.cn

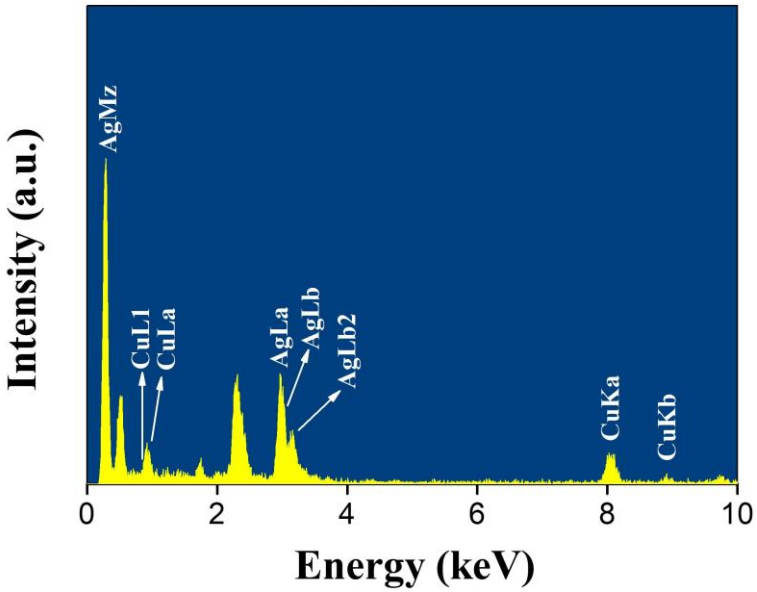

Fig. S1 EDX spectrum of the Ag_3Cu BPNs.

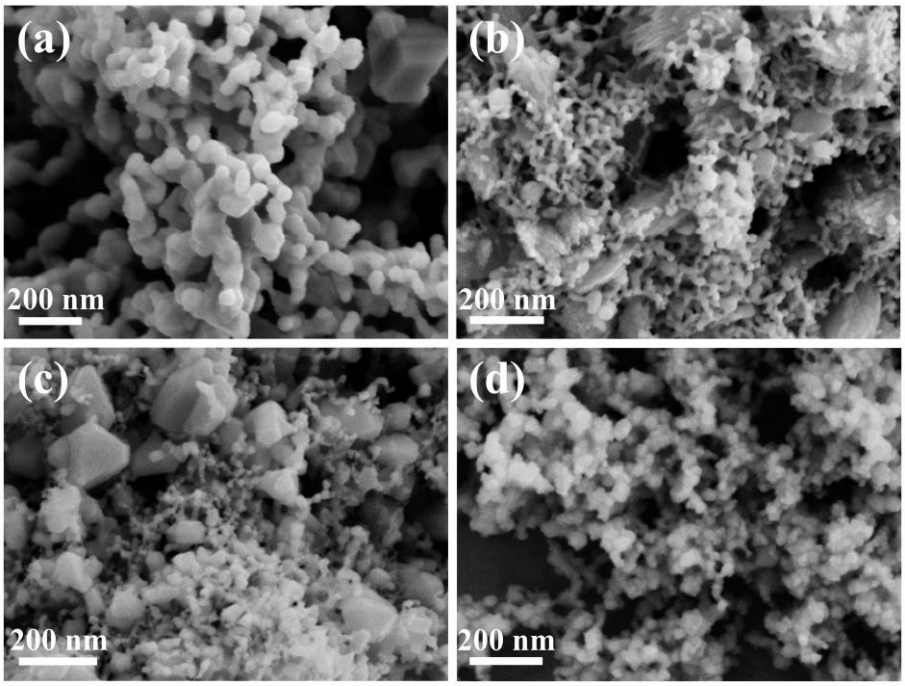

Fig. S2 SEM images of the (a) Ag, (b) AgCu, (c) $AgCu_3$, and (d) Cu nanostructures prepared under the typical synthesis condition.

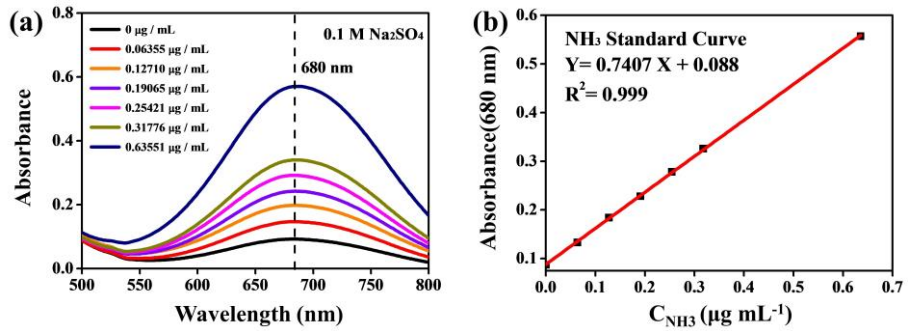

Fig. S3 (a) UV-vis curves of indophenol assays with NH_4^+ ions after incubating for 1 h at room temperature; (b) calibration curve used for estimation of NH_3 by NH_4^+ ion concentration. The absorbance at 680 nm was measured by UV-vis spectrophotometer, and the fitting curve shows good linear relation of absorbance with NH_4^+ ion concentration (Y = 0.7407X + 0.088, R^2 = 0.999) of three times independent calibration curves.

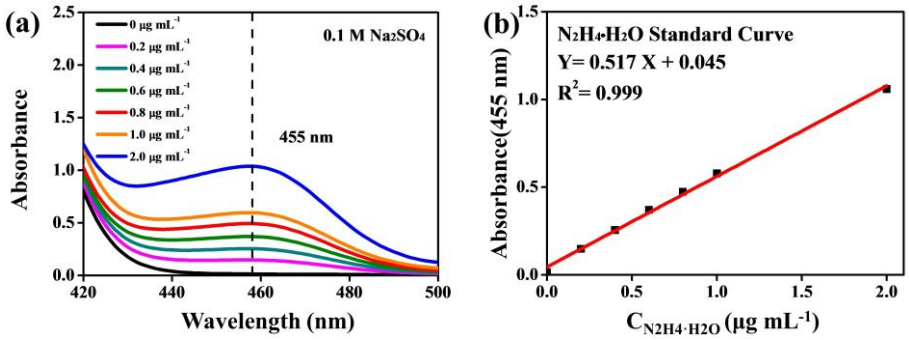

Fig. S4 (a) UV-vis curves of various $N_2H_4 \cdot H_2O$ concentration after incubating for 15 min at room temperature; (b) calibration curve used for estimation of $N_2H_4 \cdot H_2O$ concentration. The absorbance at 455 nm was measured by UV-vis spectrophotometer, and the fitting curve shows good linear relation of absorbance with $N_2H_4 \cdot H_2O$ concentration (Y = 0.517X + 0.045, R^2 = 0.999) of three times independent calibration curves.

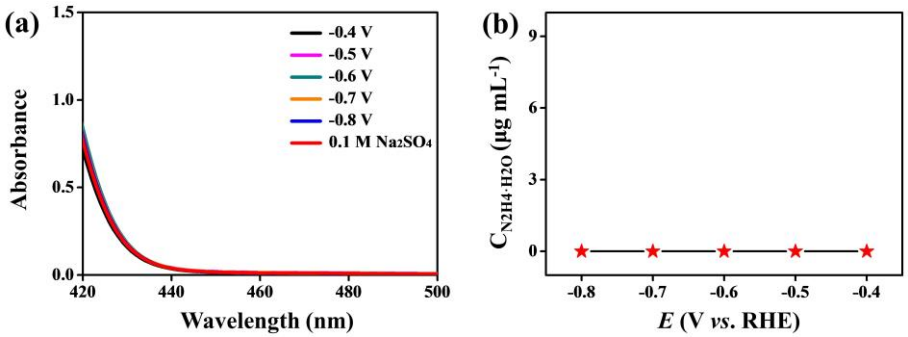

Fig. S5 The UV-vis absorption spectra and corresponding yield of N_2H_4 at selected potentials.

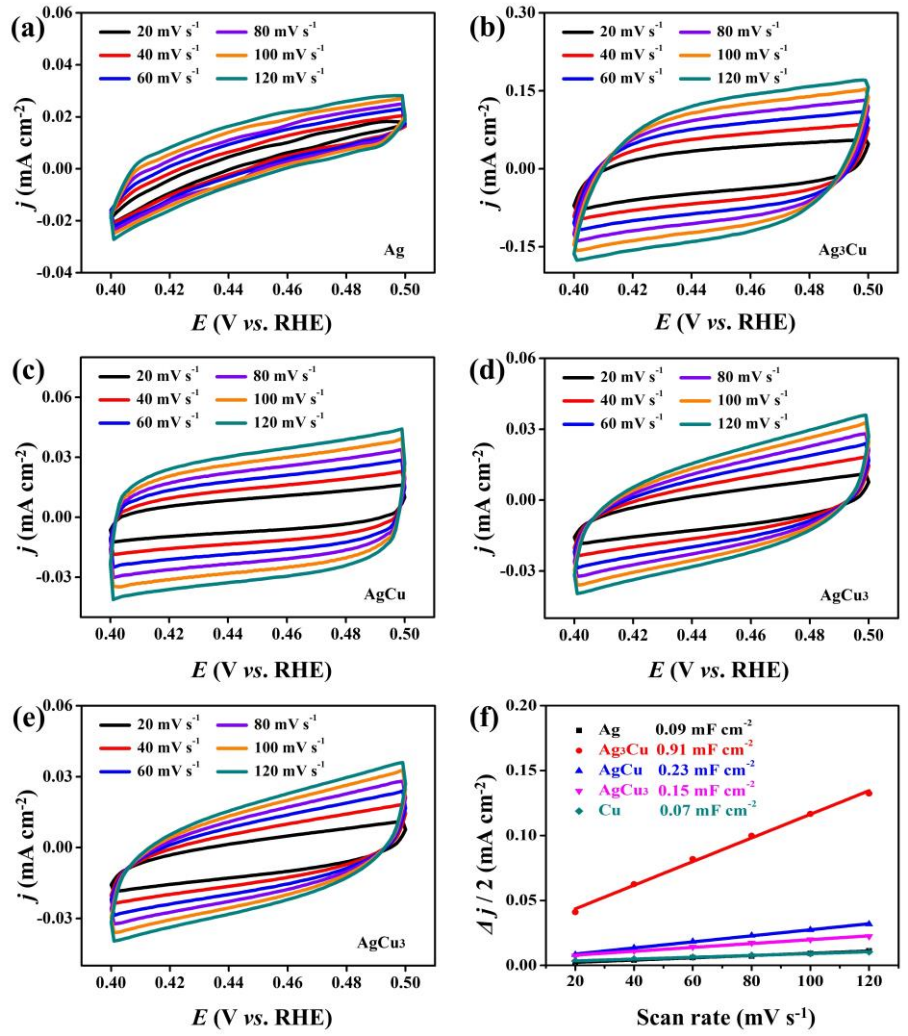

Fig. S6 (a-e) Cyclic voltammograms and (f) capacitive current densities at 0.45 V derived from CV curves against scan rate for different samples.

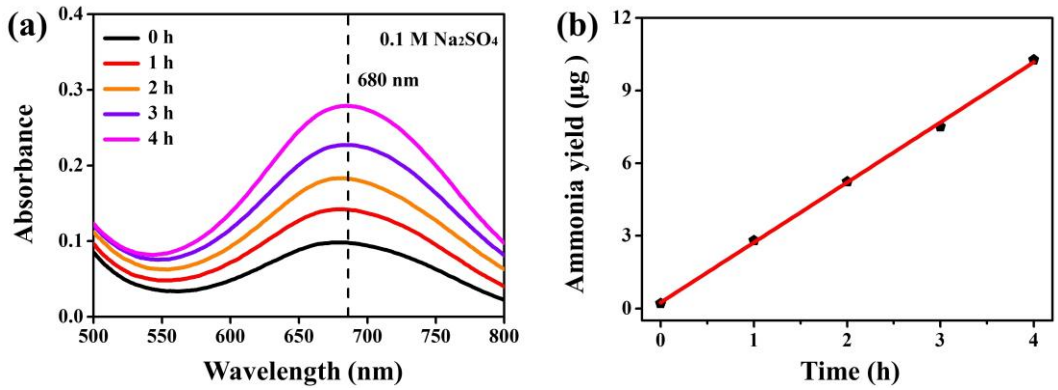

Fig. S7 (a) UV-vis absorption spectra of the electrolytes after electrolysis for different times, and (b) the relationship between the amount of ammonia formation and the electrolysis time.

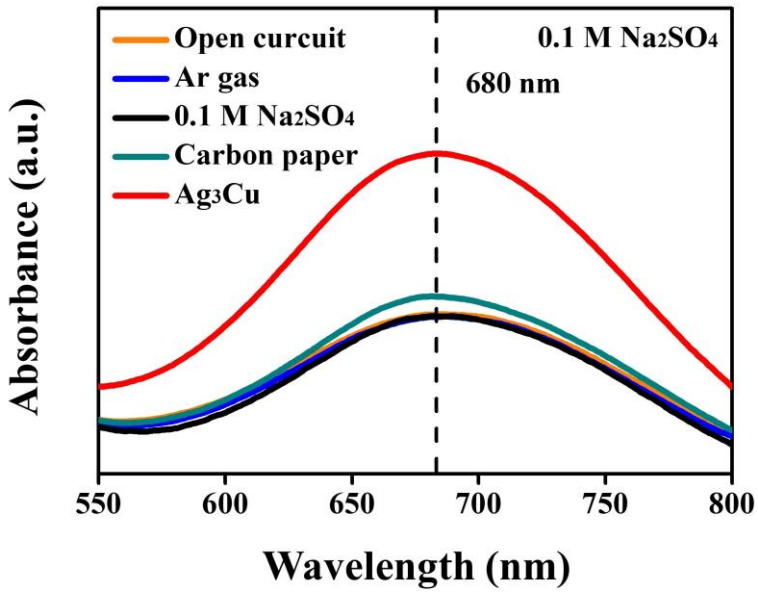

Fig. S8 UV-vis absorption spectra of the electrolytes stained with indophenols indicator under different conditions.

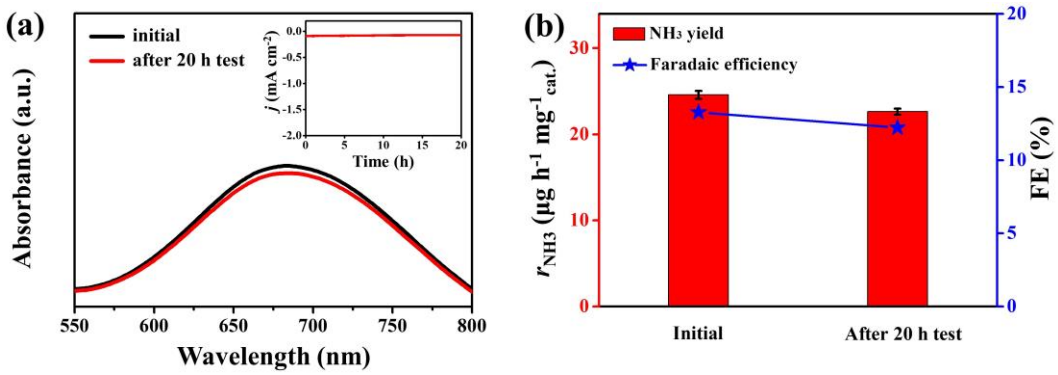

Fig. S9 (a) The long-term stability test of the Ag_3Cu BPNs for 20 h and corresponding UV-vis absorption spectra of the electrolytes before and after electrolysis. (b) the comparison of NRR performance before and after electrolysis.

Table S1. Summary of the representative catalysts on electrocatalytic NRR at ambient conditions.

Catalysts	Electrolyte	NH_3 yield rate	FE(%)	Ref.
Ag_3Cu BPNs	**0.1 M Na_2SO_4**	**24.59 μg h^{-1} $mg^{-1}_{cat.}$** **9.84 μg h^{-1} cm^{-2}**	**13.28**	**This work**
Porous bromide derived Ag film	0.1 M Na_2SO_4	1.27 μg h^{-1} cm^{-2}	7.36	[1]
Ag nanosheets	0.1 M HCl	2.83 μg h^{-1} cm^{-2}	4.8	[2]
$Pd_{0.2}Cu_{0.8}$/rGO	0.1 M KOH	2.80 μg h^{-1} $mg^{-1}_{cat.}$	~0.6	[3]
Porous PdRu	0.1 M Na_2SO_4	25.92 μg h^{-1} $mg^{-1}_{cat.}$	1.53	[4]
Fe_2O_3 nanorods	0.1 M Na_2SO_4	15.9 μg $h^{-1}$$mg^{-1}_{cat.}$	0.94	[5]
TiO_2-rGO	0.1 M Na_2SO_4	15.13 μg h^{-1} $mg^{-1}_{cat.}$	3.3	[6]
pAu/NF	0.1 M Na_2SO_4	9.42 μg h^{-1} cm^{-2}	13.36	[7]
TiO_2	0.1 M Na_2SO_4	5.61 μg h^{-1} cm^{-2}	2.5	[8]
MoS_2/CC	0.1 M Na_2SO_4	4.94 μg h^{-1} cm^{-2}	1.17	[9]
Au HNCs	0.5 M $LiClO_4$	3.90 μg h^{-1} cm^{-2}	30.2	[10]
Fe_3O_4/Ti	0.1 M Na_2SO_4	3.43 μg h^{-1} cm^{-2}	2.6	[11]
Fe_2O_3-CNT	diluted $KHCO_3$	0.22 μg h^{-1} cm^{-2}	0.15	[12]
Fe/Fe_3O_4	0.1 M PBS	0.19 μg h^{-1} cm^{-2}	8.29	[13]

References

[1] L. Ji, X. F. Shi, A. M. Asiri, B. Z. Zheng and X. P. Sun, *Inorg. Chem.*, 2018, **57**, 14692−14697.

[2] H. H. Huang, L. Xia, X. F. Shi, A. M. Asiri and X. P. Sun, *Chem. Commun.*, 2018, **54**, 11427−11430.

[3] M. M. Shi, D. Bao, S. J. Li, B. R. Wulan, J. M. Yan and Q. Jiang, *Adv. Energy Mater.*, 2018, **8**, 1800124.

[4] Z. Q. Wang, C. J. Li, K. Deng, Y. Xu, H. R. Xue, X. N. Li, L. Wang and H. J. Wang, *ACS Sustainable Chem. Eng.*, 2019, **7**, 2400−2405.

[5] X. J. Xiang, Z. Wang, X. F. Shi, M. K. Fan and X. P. Sun, *ChemCatChem*, 2018, **10**, 4530−4535.

[6] X. X. Zhang, Q. Liu, X. F. Shi, A. M. Asiri, Y. L. Luo, X. P. Sun and T. S. Li, *J. Mater. Chem. A*, 2018, **6**, 17303–17306.

[7] H. J. Wang, H. J. Yu, Z. Q. Wang, Y. H. Li, Y. Xu, X. N. Li, H. R. Xue and L. Wang, *Small*, 2019, **15**, 1804769.

[8] R. Zhang, X. Ren, X. F. Shi, F. Y. Xie , B. Z. Zheng, X. D. Guo and X. P. Sun, *ACS Appl. Mater. Interfaces*, 2018, **10**, 28251−28255.

[9] L. Zhang, X. Q. Ji, X. Ren, Y. J. Ma, X. F. Shi, Z. Q. Tian, A. M. Asiri, L. Chen, B. Tang and X. P. Sun, *Adv. Mater.*, 2018, **30**, 1800191.

[10] M. Nazemi, S. R. Panikkanvalappil and M. A. El-Sayed, *Nano Energy*, 2018, **49**, 316−323.

[11] Q. Liu, X. X. Zhang, B. Zhang, Y. L. Luo, G. W. Cui, F. Y. Xie and X. P. Sun, *Nanoscale*, 2018, **10**, 14386−14389.

[12] S. Chen, S. Perathoner, C. Ampelli, C. Mebrahtu, D. Su and G. Centi, *Angew. Chem., Int. Ed.*, 2017, **56**, 2699−2703.

[13] L. Hu, A. Khaniya, J. Wang, G. Chen, W. E. Kaden and X. F. Feng, *ACS Catal.*, 2018, **8**, 9312–9319.